

Eulerian flow velocities in the swash zone: Field data and model predictions

Michael G. Hughes

School of Geosciences, University of Sydney Institute of Marine Science, University of Sydney, Sydney, New South Wales, Australia

Tom E. Baldock

Department of Civil Engineering, University of Queensland, Brisbane, Queensland, Australia

Received 19 November 2003; revised 28 April 2004; accepted 24 May 2004; published 13 August 2004.

[1] Measurements of Eulerian flow velocity obtained within the swash zone on a relatively steep beach face (gradient 1:23) are compared with an extended ballistic swash model. The model only requires a friction factor, beach slope and terminal bore velocity as input. The following model predictions matched well with observations: (1) The maximum Eulerian flow velocity is the shoreline velocity when it arrives at the fixed point of interest on the beach face; (2) at any location the time of flow reversal occurs prior to the shoreline reaching its maximum landward excursion; (3) the maximum flow velocity in the backwash is the velocity recorded as the shoreline recedes past the fixed point of interest (and this is less than the maximum uprush velocity); and (4) the duration of the uprush flow is shorter than the duration of the backwash flow. Previous studies have already confirmed that the ballistic swash model (including friction) can accurately predict shoreline motion and maximum run-up on steep beaches. This study shows that it is similarly successful in predicting Eulerian flow velocities during individual swash events. The model does not presently account for interacting swash, however, and so may be less appropriate on gently sloping beaches. **INDEX TERMS:** 4546 Oceanography: Physical: Nearshore processes; 4560 Oceanography: Physical: Surface waves and tides (1255); 4568 Oceanography: Physical: Turbulence, diffusion, and mixing processes; **KEYWORDS:** swash, flow velocity, beach face

Citation: Hughes, M. G., and T. E. Baldock (2004), Eulerian flow velocities in the swash zone: Field data and model predictions, *J. Geophys. Res.*, 109, C08009, doi:10.1029/2003JC002213.

1. Introduction

[2] The swash zone is typically defined as that zone landward of the surf zone where the shoreline sweeps back and forth across the beach in response to the passage of waves. The hydrodynamics within the swash are important, because a substantial part of the total littoral sediment transport occurs in this zone. Suspended sediment concentrations and sediment transport rates in the swash are generally well in excess of those measured elsewhere in the surf zone [e.g., Osborne and Rooker, 1999; Masselink and Hughes, 1998]. In comparison to the surf zone, swash zone hydrodynamics are relatively poorly understood. This is due in part to the difficulties of data acquisition in intermittent, shallow, bubbly, and rapidly varying flows, which makes data analysis and critical comparisons between theory and observations more difficult. As a result, there are very limited data on swash zone fluid velocities, and only one previous study comparing field observations (from a gently sloping dissipative beach) with theoretical calculations [Raubenheimer, 2002].

[3] This paper addresses this point by presenting comparisons between new field observations from an intermediate-

reflective beach face and predictions from an extended ballistic swash model. Data-model comparisons include water depths, flow velocities, and flow durations. In particular, detailed comparisons between measured and predicted Eulerian flow velocities are presented for individual swash events from different relative positions within the swash zone. No such comparisons have previously been published in the literature. Given two recent comprehensive reviews of field measurements [Butt and Russell, 2000], swash hydrodynamics, and sediment transport [Elfrink and Baldock, 2002], section 2 provides a brief overview of relevant previous work together with some important definitions relevant to the later parts of this paper. Section 3 describes the theoretical background and development of the numerical model, and section 4 provides a description of the field site and data analysis techniques. Section 5 presents and compares the field data with model calculations. A further discussion of the data, model results, and a sensitivity analysis are given in section 6, followed by final conclusions.

2. Previous Work

[4] A swash cycle is defined as commencing when the shoreline begins moving landward due to the arrival of a

wave and ending after the shoreline has retreated back to its original position, or to a point where the following wave begins to push the shoreline landward again. A swash cycle consists of two components: (1) the uprush, which is when the shoreline is moving landward and (2) the backwash, which is when it is moving seaward. The total time interval is the individual swash period. The motion of the shoreline is usually measured by resistance wires (run-up wires) placed parallel to the bed or by video [Holman and Guza, 1984; Holland *et al.*, 1995]. These techniques yield continuous data measured within a Lagrangian reference frame. Pressure transducers or current meters measuring at a fixed point within the swash lens, however, only yield data within a Eulerian reference frame, with discrete flow events separated by time periods when water is absent. Hence a swash event is defined as the flow recorded at a fixed location of interest on the beach (i.e., the local swash measured in an Eulerian reference frame), and the flow duration is that period when water is present at that location.

[5] On relatively steeply sloping beaches, waves often arrive at the exposed beach face at roughly the same location, and the ensuing swash cycle is largely or entirely complete before the following wave arrives; that is, the swash period is equal to or shorter than the wave period. In this instance the swash cycle commences when the incoming bore reaches the exposed beach face and finishes when the shoreline returns to the original position, such that the resulting motion is well suited to a wave-by-wave analysis [e.g., Shen and Meyer, 1963; Waddell, 1976; Yeh *et al.*, 1989; Hughes *et al.*, 1997; Baldock and Holmes, 1997; Peregrine and Williams, 2001; Puleo *et al.*, 2003]. In contrast, on gently sloping beaches the waves arrive at the beach face over a broad zone, and there is frequent interaction between the next incident short wave and the preceding swash. The location at which bores encounter the exposed beach and where an individual swash cycle begins occurs anywhere over a zone tens of meters wide. Toward the seaward limit of the swash zone in particular, the time period between the beach emerging is then of the order of the period of any long waves present in the surf zone [e.g., Holland *et al.*, 1995; Butt and Russell, 1999; Raubenheimer, 2002]. Eulerian flow velocities measured in the swash zone on these beaches consist of events resulting from both individual short waves and events with multiple short waves overrunning the preceding swash, together with any underlying long wave motion. This type of data is less well suited to an event-by-event analysis.

[6] In recent years the paradigm for field-based swash research on both steep and gently sloping beaches has almost exclusively been nonlinear shallow water theory. For example, Hughes [1992], Raubenheimer *et al.* [1995], and Raubenheimer and Guza [1996] used this theoretical context in their studies of shoreline motion, maximum run-up height, and the dynamic shape of the swash lens. The former compared field data with a ballistic swash model originally developed by Shen and Meyer [1963] and the latter two tested the RBREAK model originally developed by N. Kobayashi and colleagues [e.g., Kobayashi and Wurjanto, 1992]. The shoreline motion described by the ballistic model is an analytical solution to the one-dimensional, depth-averaged, nonlinear shallow

water equations (NLSWE), which is applicable to bores approaching the shoreline, but it cannot account directly for interactions between swash events. It is therefore most applicable to discrete swash events, more typical on steeper beaches. Conversely, the RBREAK model solves the governing NLSWE numerically, with input conditions outside the breakpoint. Raubenheimer [2002] concluded that on a mildly sloping beach the RBREAK model provided good estimates of the cross-shore structure of orbital velocity magnitudes and nonlinear characteristics, but that velocity skewness and the ratio of local uprush to backwash flow durations were overpredicted. To our knowledge, local flow velocity predictions from either the ballistic model or RBREAK have yet to be compared with field data from steeper beaches.

3. Model Background and Development

[7] The numerical model developed here is based on the analytical solution for the shoreline motion proposed by Shen and Meyer [1963], combined with a quadratic friction law applied to the run-up tip and a semi-empirical function describing the flow depths within the swash lens. In an inviscid flow, Shen and Meyer [1963] showed that for fully developed turbulent bores the shoreline motion is dependent only on the bore velocity upon arrival at the initial shoreline position, which subsequent laboratory experiments have shown is accurate [Yeh *et al.*, 1989]. The motion of the front of the swash lens (moving shoreline) and some details of the flow within the swash lens can be determined from a set of assumptions and corollaries of the NLSWE [Shen and Meyer, 1963]. Ho *et al.* [1963] described a useful way to visualize the mathematical arguments by imagining that the swash lens consists of several small fluid elements, each containing the same mass of water at all times. The motion of each fluid element depends only on the pressure exerted by the adjacent elements and gravity. Freeman and LeMehaute [1964] argued that the swash lens is analogous to a rarefaction wave; thus the leading element is always moving faster than the elements behind, and the pressure acting on it will be negligible.

[8] The problem of the shoreline climbing the beach therefore simplifies to a consideration of the balance of forces acting on the leading element alone. Including friction due to a bed shear stress, the depth-averaged equation of motion for the shoreline (which is analogous to ballistic motion) is therefore

$$m \frac{d^2 X}{dt^2} + mg \sin \beta + \tau \delta = 0, \quad (1)$$

where m is the mass of the fluid element, X is its position relative to the initial shoreline position, $x = 0$, t is time relative to the time of bore collapse at $t = 0$, g is the gravitational acceleration, β is beach slope, τ is the bed shear stress, and δ is the nominal length (and also depth) of the fluid element. The bed shear stress is usually approximated using a quadratic friction law,

$$\tau = \frac{1}{2} \rho f \left| \frac{dX}{dt} \right|, \quad (2)$$

where ρ is the fluid density, f is the friction factor, and dX/dt is the shoreline velocity. Substituting equation (2) into equation (1) and dividing throughout by $m = \rho\delta^2$ yields

$$\frac{d^2X}{dt^2} + g \sin \beta + \frac{f}{2\delta} \frac{dX}{dt} \left| \frac{dX}{dt} \right| = 0. \quad (3)$$

[9] If g , β , f , and δ are assumed to be constants, then equation (3) can be solved analytically for the shoreline position X through time. The initial conditions at $t = 0$ are: (1) The shoreline velocity, $U = dX/dt$, is equal to the terminal bore velocity u_o , and (2) the shoreline position X is located at $x = 0$. Integrating equation (3) twice using separation of variables yields the shoreline position during the uprush X_u [Kirkgöz, 1981; Hughes, 1995],

$$X_u = \frac{2\delta}{f} \ln \left[\frac{\cos(At + B)}{\cos B} \right], \quad (4)$$

where

$$A = -\sqrt{\frac{gf \sin \beta}{2\delta}} \quad \text{and} \quad B = \tan^{-1} \left(\frac{u_o \sqrt{f}}{\sqrt{2g\delta \sin \beta}} \right). \quad (5)$$

The use of equation (4) is only valid until the shoreline has reached its maximum displacement landward (i.e., when $dX_u/dt = 0$). Hughes [1995] showed that the time that this occurs, t_{\max} (equivalently the uprush duration), is given by

$$t_{\max} = B/A, \quad (6)$$

and the position of maximum shoreline displacement X_{\max} is given by

$$X_{\max} = \frac{-2\delta}{f} \ln(\cos B). \quad (7)$$

The shoreline position during the backwash is also obtained from equation (3). The initial conditions at $t = 0$ for the backwash are: (1) The shoreline velocity is equal to zero, and (2) the shoreline position X is again defined as $x = 0$. Again, integrating equation (3) twice yields the shoreline position during the backwash X_b , which measured relative to X_{\max} is [Holland and Puleo, 2001]

$$X_b = -\frac{2\delta}{f} \ln[\cosh At]. \quad (8)$$

Note that the values of f and δ may differ during the uprush and backwash. Equations (4) and (8) assume a constant bed slope within the swash zone, which may not always be a good approximation, particularly on steep bermed beaches. In this instance, the variable beach slope can be accounted for by evaluating equation (1) numerically using simple finite differences to obtain both dX/dt and X throughout the swash cycle. For simplicity, however, the model is applied here assuming a plane slope.

[10] An estimate of the depth averaged Eulerian flow velocity $u(t)$ at any fixed location of interest $x = x_i$ on the beach face can be obtained using the mass balance principle,

where the discharge of water Q (per unit width of beach) that passes x_i is [Hughes, 1989; Turner and Masselink, 1998; Peregrine and Williams, 2001]

$$Q = \frac{V}{t} = hu, \quad (9)$$

and V is the time-varying volume of water up beach from x_i . In order to obtain a practical expression for u , we need an expression for the water depth h as a function of both time and distance. In the inviscid model, the water depth varies as [Shen and Meyer, 1963; Peregrine and Williams, 2001]

$$h(x, t) = \frac{(X - x)^2}{9gt^2}. \quad (10)$$

Equation (10) is only valid close to the run-up tip, however, and predicts a thin concave-up swash profile that is expected to be dominated by friction effects. Consistent with this, field and laboratory studies have shown that equation (10) is not accurate over much of the swash zone, and that a convex water surface profile occurs during the uprush [Hughes, 1992; Raubenheimer et al., 1995]. Baldock and Holmes [1997] proposed a semi-empirical formulation for h that more closely approximates experimental observations,

$$h(x, t) = H_b \left(\frac{X - x}{X} \right)^C \left(\frac{T_s - t}{T_s} \right)^D, \quad (11)$$

where H_b is the terminal bore height, T_s is the swash period, and C and D are empirical coefficients. Equation (11) is based on the following constraints: (1) when $(X - x) \leq 0$, then $h = 0$; (2) when $x = 0$ and $t = 0$, then $h = H_b$; and (3) when $x = 0$ and $t = T_s$, then $h = 0$ (i.e., the water depth is equal to the height of the incident bore at the start of the uprush, $x = 0$, reducing to zero at the end of the backwash and at the run-up tip). This formulation assumes that individual noninteracting swash events have a similar water surface profile, dependent on fixed choices of C and D for particular wave conditions and beach slope. The sensitivity of the model to these choices is discussed later in the context of the experimental data. Note that equation (11) describes the flow depth from the start of bore collapse, i.e., with an initially vertical front face. The volume of water shoreward of the fixed location of interest $x = x_i$ is

$$V = \int_{x_i}^X h \cdot dx. \quad (12)$$

Re-arranging equation (9) and expressing it in finite difference form yields the following equation for the Eulerian flow velocity u at $x = x_i$:

$$u = \frac{V(t + \Delta t) - V(t - \Delta t)}{2h(t)\Delta t}, \quad (13)$$

where $h(t)$ is obtained from equation (11) and $V(t \pm \Delta t)$ is obtained from equation (12). Baldock and Holmes [1997]

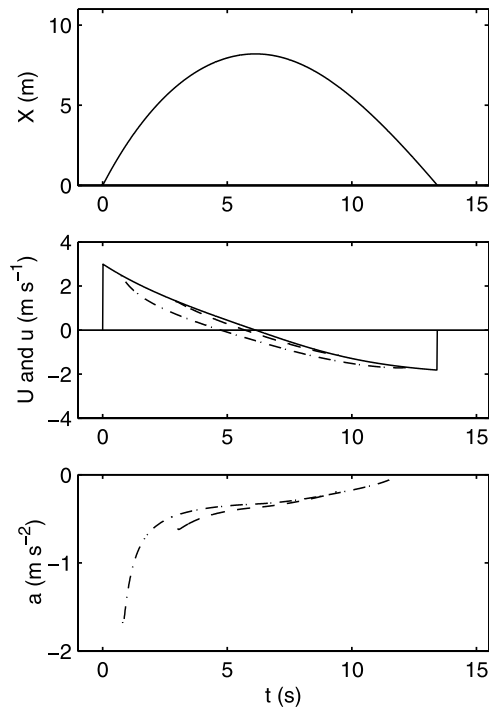


Figure 1. An example of swash behavior predicted by the viscous ballistic swash model. From top to bottom the shoreline position $X(t)$, the shoreline velocity $U(t)$ (solid line) and the local flow velocity $u(t)$ at two locations on the beach: $x = 2$ m (dash-dotted line) and $x = 6$ m (dashed line), and the corresponding Eulerian flow accelerations $a = \partial u / \partial t$. Initial conditions used in the example are described in the text.

demonstrate good agreement between equations (11) and (13) and laboratory data for both fluid velocities and flow depths in the swash zone.

[11] Predictions of the viscous ballistic swash model for the shoreline position, X , shoreline velocity, U , Eulerian flow velocity, u , and local temporal acceleration, $a = \partial u / \partial t$, at two locations in the swash are shown in Figure 1. The following input conditions were used in the model: initial swash velocity $u_o = 3 \text{ m s}^{-1}$, beach gradient $1/23$, friction factor for the uprush $f_u = 0.007$, and friction factor for the backwash $f_b = 0.04$. These values for the friction factors are in the middle of the range of those proposed by *Puleo and Holland* [2001]. The maximum swash depth at the mid swash position is used here to represent δ_u during the uprush [Hughes, 1995], which is obtained by evaluating equations (4) and (11) iteratively. The backwash value δ_b was set to $0.6\delta_u$ [Puleo and Holland, 2001].

[12] The path of the shoreline is asymmetric, and the maximum landward displacement of the shoreline and the swash period are reduced in comparison to the inviscid solution of equation (1). The maximum shoreline velocity during uprush is equal to the terminal bore velocity, u_o , but the maximum shoreline velocity at the end of the backwash is reduced by friction. Note that the shoreline velocities at the beginning and end of the swash cycle are shown to start at and return to zero (middle panel of Figure 1). This is because, at those times, the shoreline is stationary and

located at $x = 0$. The first and last Eulerian flow velocity observed at any fixed location on the beach is the shoreline velocity at that location; prior to and after the swash event the velocity is undefined, not zero. The model also predicts that the flow velocity at any point seaward of the run-up limit reverses prior to the time of maximum run-up. This diverging flow has been widely observed [e.g., *Larson and Sunamura*, 1993; *Baldock and Holmes*, 1997], and is also predicted by numerical calculations of both inviscid swash [Hibberd and Peregrine, 1979] and with friction included [Raubenheimer and Guza, 1996]. It is an important feature of the swash kinematics, leading to the rapid thinning of the swash lens around the time of maximum uprush. Notice that at any fixed location on the beach the local temporal flow acceleration, $\partial u / \partial t$, throughout the swash is predicted to be negative (bottom panel of Figure 1).

[13] In theory, the swash cycle from the first bore must be complete prior to arrival of the following bore, and therefore the ballistic swash model cannot explicitly account for swash interaction. Nevertheless, even with interaction between swash cycles, it can provide a very good approximation to the shoreline motion if individual short waves drive the swash uprush [Baldock and Holmes, 1999]. Here, however, the model is applied to conditions with minimal or no interaction between swash cycles (see sections 4 and 5).

4. Field Data and Analysis Techniques

4.1. Study Site

[14] North Stradbroke Island is a barrier sand island located off the Queensland coast, Australia. The seaward side of the island is exposed to a moderate energy, swell wave climate. The modal surf zone morphology varies between the “longshore bar trough” and “transverse bar and rip” beach states defined by *Wright and Short* [1984]. Swash oscillations at short wave frequencies are driven by breaking waves, which make the site suitable for investigating swash forced by collapsing turbulent bores. The surf zone gradient was $1:55$, and the mean beach face gradient was $1:23$, which was assumed planar for numerical modeling purposes. Sediment size on the beach face was in the medium sand range with a median diameter of 0.28 mm .

4.2. Instrumentation and Data Processing

[15] Locations of instruments used in the experiment are shown on the beach profile in Figure 2. A Nortek sideways-looking acoustic Doppler velocimeter (ADV) was used to measure the shore-normal flow velocity tangential to the bed, with the sampling volume maintained $1.5\text{--}2.5 \text{ cm}$ above the bed by an observer. A Druck PTX1830 pressure sensor was used to measure swash depth at the ADV location. The shoreline location was measured with a run-up wire, again maintained $1\text{--}2 \text{ cm}$ above the bed. A second pressure sensor measured incident wave conditions in the inner surf zone. Instruments were logged at 10 Hz for 3.5 hours at the top of the tide. The location of bore collapse varied due to both infragravity and tidal fluctuations in the water level, providing data from a wide variety of positions within the swash zone. Swash cycles were selected for analysis if there was no interaction, or if interaction was limited to the last 10% of the swash cycle and occurred well

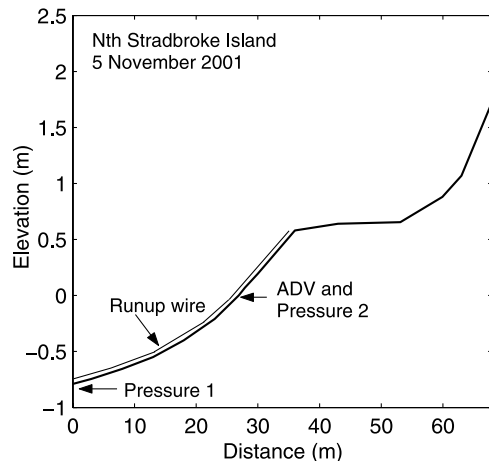


Figure 2. Surveyed beach profile from the experiment site showing the instrument positions. Vertical exaggeration is 16, and the beach face slope angle is 2.5° .

seaward of the ADV station. This was assessed by visual inspection of the run-up wire and pressure sensor records; the requirement was no secondary maximum in the local water depth record and no shoreline overrunning <2 m seaward of the ADV. A total of 214 such events had reliable data from all three instruments and were selected for the analysis below. These events represent 55% of the swash cycles that passed the ADV. In the remainder, either significant swash interaction occurred (20%) or the ADV signal was too noisy for an accurate assessment of the data (25%; see below).

[16] An example of the data obtained for a single swash event is shown in Figure 3. The time series of shoreline position X obtained from the run-up wire was used to delimit the period of the swash cycle T_s . The uprush starts at the time of bore collapse ($t = 460.4$ s) and continues to the time the shoreline reaches its maximum landward excursion ($t = 464.0$ s). At this time the backwash starts and continues until the shoreline recedes to its maximum seaward excursion and becomes almost stationary again ($t = 470.0$ s). The time series of swash depth h obtained from Pressure 2 was used to delimit the flow durations for the swash events at the ADV, with uprush, T_u , and backwash, T_b , durations defined using the zero-crossing velocity obtained from the ADV. The swash pressure transducer was used to determine the exact time that the shoreline (swash tip) passed the ADV. The shoreline velocity, $U = dX/dt$, was obtained at the same instant in time from the run-up wire record, which assumes that the run-up wire record accurately represents the shoreline motion at the bed elevation. Holland *et al.* [1995] suggest that this will be the case and that any errors will be minor provided the run-up wire height is less than a few centimeters, which was certainly the case here. The absolute position of the shoreline during the latter stages of the backwash is more difficult to determine, since the water surface approaches the beach slope and the water depth is very shallow. It is therefore difficult to compare accurately the ADV velocity and shoreline velocity at the same instant in time, and this is not attempted here.

[17] ADV velocity measurements exhibit significant noise in highly turbulent and/or aerated flow with large

suspended sediment concentrations. Moreover, the signal fluctuates widely around a zero mean when the instrument is out of the water. Hence, following Elgar *et al.* [2001], who proposed a threshold ADV signal correlation condition based on the sampling frequency, s_f (correlation $> 0.3 + 0.4\sqrt{s_f/25}$), velocity data were rejected when the signal correlation for a particular beam was $<55\%$ (Figure 3). Consequently, the velocity records for individual swash events are truncated to varying degrees near the start, due to excessive acoustic scatter in the leading edge of the swash lens and near the end due to the backwash flow dropping below the height of the ADV (indicated by vertical lines on the lower panels of Figure 3). On this basis the apparent flow acceleration and deceleration evident in the raw velocity signal are excluded since the data do not satisfy the quality threshold. Note that the velocity record in the bottom panel of Figure 3 is not zero between swash events; it is undefined when no water is present.

5. Results

[18] Significant energy was observed in both the gravity and infragravity wave bands in the inner surf zone (Figure 4). Consistent with many previous observations of swash, the beach face acted as a low-pass filter, with the run-up (shoreline oscillation) displaying a downshifting of

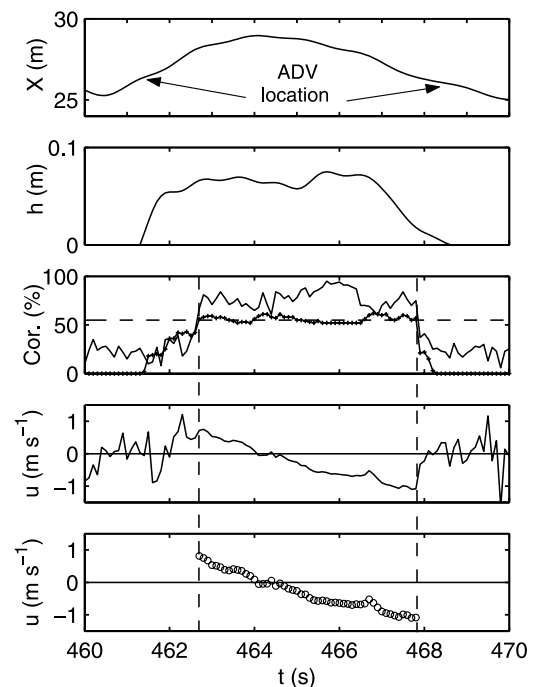


Figure 3. Example of a single swash event showing (from top to bottom) time series of the shoreline position X measured by the run-up wire (with location of ADV at $x = 26.3$ m also indicated), the local swash depth h measured by the pressure transducer, the signal correlation (Cor., solid line) and signal-to-noise ratio (SNR, crosses) of the ADV acoustic beam, the unprocessed horizontal velocity record u (solid line), and the processed record (open circles). The vertical dashed lines through the bottom three panels delimit reliable ADV data.

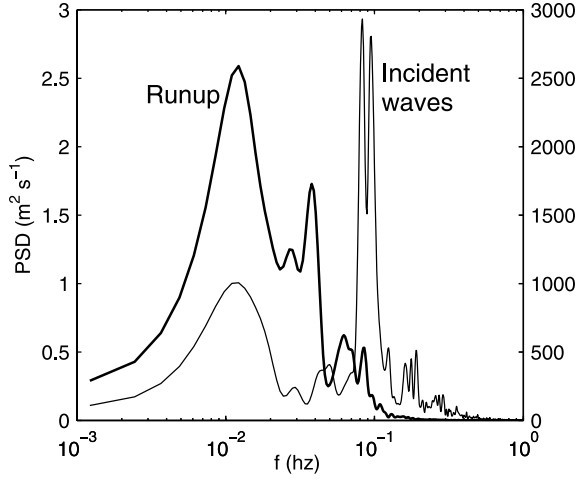


Figure 4. Typical power spectrum for the incident waves in the inner surf zone measured at Pressure 1 (left-hand axis), and the shoreline oscillations measured by the run-up wire (right-hand axis). Both spectra have 30 degrees of freedom.

the peak frequency in the gravity band and the infragravity band assuming predominance. Consequently, a mix of breaking and nonbreaking waves may be present in the swash data. Nevertheless, each swash cycle analyzed here is associated with turbulent, fully developed bores collapsing on arrival at the exposed beach face. The extent to which any underlying long waves might affect the incident bores or individual short wave run-up is unknown and a subject for further research beyond the scope of this paper. Incident bores had a significant height of 0.35 m and peak spectral period of 11 s. The average height of the highest 10% of bores was 0.55 m.

[19] The reliable flow velocity measurements (with acoustic signal correlation $>55\%$) for all 214 swash events are shown in the panels on the left-hand side of Figure 5. Velocities have been normalized against the velocity of the shoreline as it passes the ADV, and time has been normalized against the local flow duration ($T_u + T_b$). The data are grouped according to the normalized position of the ADV within the shoreline excursion for each swash event (i.e., the distance of the ADV from the start of the swash divided by the shoreline excursion length, X_{\max}). The top, middle, and bottom panels include swash events in the ranges $0.125-0.375X_{\max}$, $0.375-0.625X_{\max}$, and $0.625-0.875X_{\max}$, respectively. Ensemble-averaged flow velocities from all 214 swash events are shown in the adjacent panels on the right-hand side of Figure 5. These were obtained by dividing the normalized time into bin widths of 0.1 and averaging all the velocities within each bin.

[20] The ensemble-averaged velocity data in Figure 5 were then used to calibrate the ballistic swash model presented in section 3. The free parameters in the model are δ_u , δ_b , f_u , and f_b in equations (4) and (8), and C and D in equation (11). The values of C and D were set to 0.75 and 1, respectively, and δ_u and δ_b were calculated iteratively within the model as outlined in section 3. Individual model runs with different friction factor values were then performed until the best match was achieved to the ensemble-averaged

velocity data at the mid-swash position (middle panel in Figure 5). The resulting friction factors obtained for this data set were $f_u = 0.01$ and $f_b = 0.05$. The good comparison between the measured ensemble-averaged velocities and the calibrated model predictions at the other more seaward and landward locations suggests that these friction factors are applicable over the majority of the swash zone.

[21] Figure 6 shows direct model versus data comparisons for 10 randomly selected individual swash events. In all cases the free parameters and friction factors were set to the values stated in the previous paragraph. The remaining model inputs were the beach face gradient, $\beta = 1/23$, and the initial shoreline velocity, u_o , obtained from the run-up wire. The bore height H_b at the initial shoreline, required in equation (11), was hindcast using the usual relationship $u_o = 2\sqrt{gH_b}$. The distance from the initial shoreline position to the ADV, x_i , is indicated for each event. The earliest velocity measurement shown in each swash event is the shoreline velocity when it arrived at the ADV. In most cases, both the timing and magnitude of the shoreline velocity at the ADV location match closely with model predictions. Similarly, in most examples the general shape and magnitude of the velocity time series throughout the swash event matches very well with predictions. In many cases the model predictions at the end of the swash event extend beyond the data. This is because the water level in the backwash has dropped below the ADV or the signal quality threshold was not satisfied. In all cases the measurements show no deceleration of the local backwash velocity

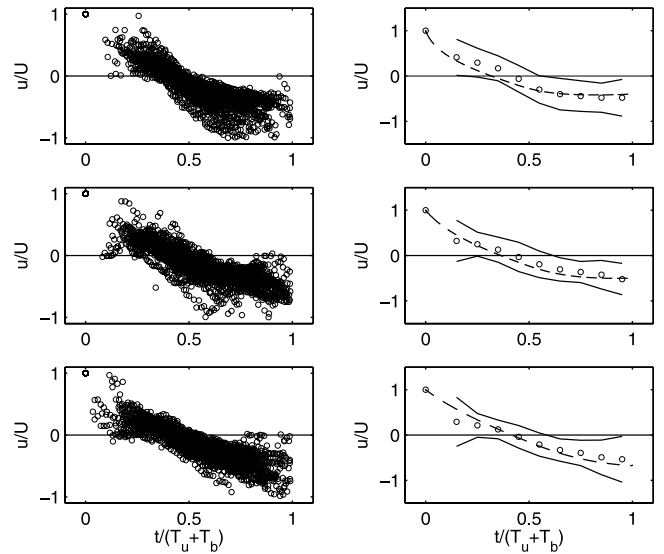


Figure 5. (left) Normalized flow velocity measurements (only those with signal correlations $>55\%$) for all 214 swash events grouped according to the position of the ADV relative to the shoreline excursion length. (top) Swash events where the relative position of the ADV is in the range $0.125-0.375X_{\max}$, (middle) those in the range $0.375-0.625X_{\max}$, and (bottom) those in the range $0.625-0.875X_{\max}$. Adjacent panels on the right-hand side show the ensemble-averaged velocities (circles) and ± 2 standard deviations (solid lines). Also shown are best fit calibrated results from the ballistic swash model including friction (dashed lines).

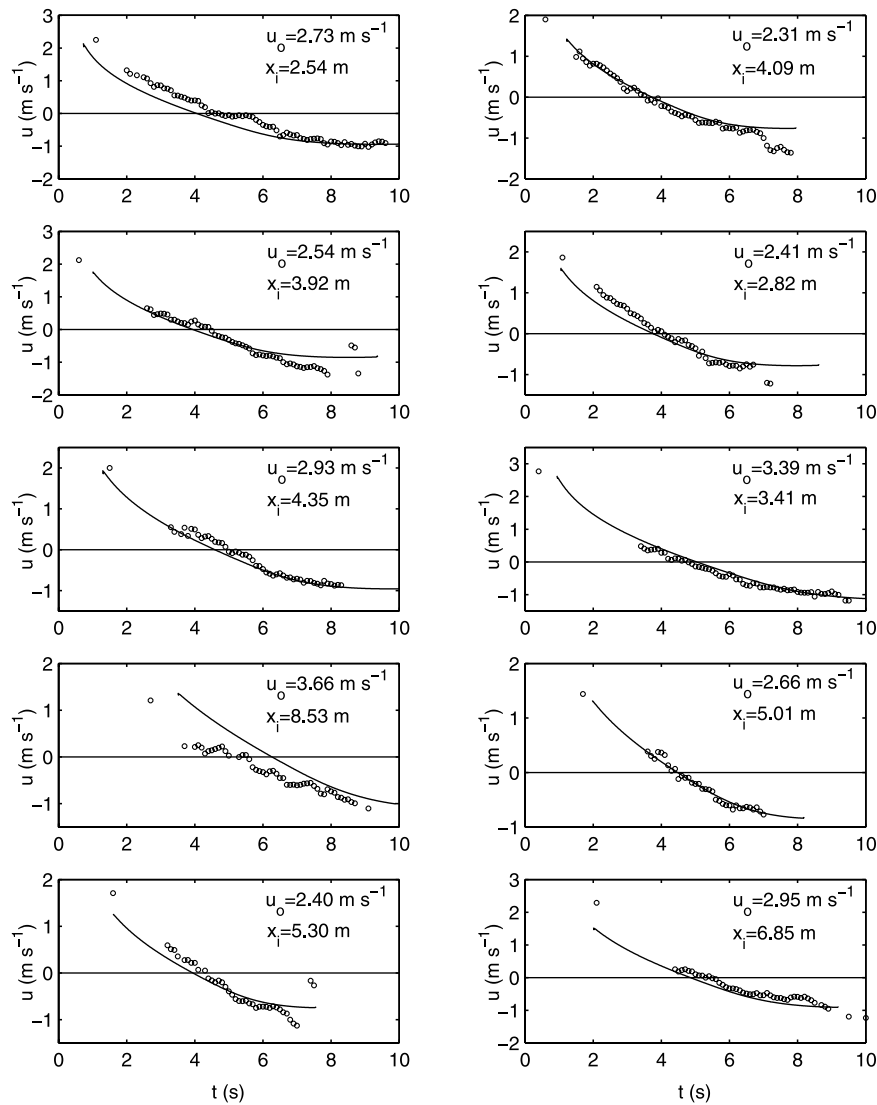


Figure 6. Measured Eulerian flow velocity (open circles) compared with model predictions (solid line) for 10 individual swash events. The values for shoreline velocity at the beginning of the swash cycle u_0 (i.e., the terminal bore velocity) and distance of the ADV from the shoreline position at the beginning of the swash cycle x_i , used to initialize the model in each case, are also shown.

prior to the end of the swash event, consistent with the model predictions. Note that this may not be the case if swash interaction occurs, i.e., if the next incoming bore passes the measurement location before the preceding swash depth reduces to zero.

[22] The fact that the model predictions for depth-averaged horizontal velocity sit well within 2 standard deviations about the ensemble averages of the data (Figure 5) qualitatively suggests that the model performs well across the entire data set. Nevertheless, the root-mean-square (RMS) error between data and model predictions for both swash depth and velocity for all 214 swash events (compare Figures 6 and 10) were also calculated, and the frequency distributions of both are shown in Figure 7. The modal RMS errors for the model predictions of depth and velocity are 0.03 m and 0.2 m s $^{-1}$, respectively, and for most of the data set the RMS error in the velocity is restricted to ≤ 0.4 m s $^{-1}$. Note that the model-data comparisons are

relative to the start of the swash cycle, i.e., from the time of bore collapse when the shoreline starts moving shoreward (see Figure 1). This is a severe test of the model capabilities, effectively a comparison of the phase match between predicted and measured data, not just the magnitude or temporal variation. In general, the model tends to overestimate the flow velocity in the backwash (Figure 5), which is partly due to phase errors, but may be also a result of comparing depth averaged velocity predictions with measurements made close to the bed. If a roughly logarithmic boundary layer exists, then data from *Raubenheimer et al.* [2004] suggest that the ratio of near bed flow velocity to depth-averaged flow velocity will be approximately 0.8–0.9.

[23] A key feature of the internal swash kinematics is asymmetry in uprush/backwash flow durations and velocities, with many previous laboratory and field studies showing that $T_u < T_b$ [e.g., *Kemp, 1975; Raubenheimer et al., 1995; Baldock and Holmes, 1997; Masselink and Hughes,*

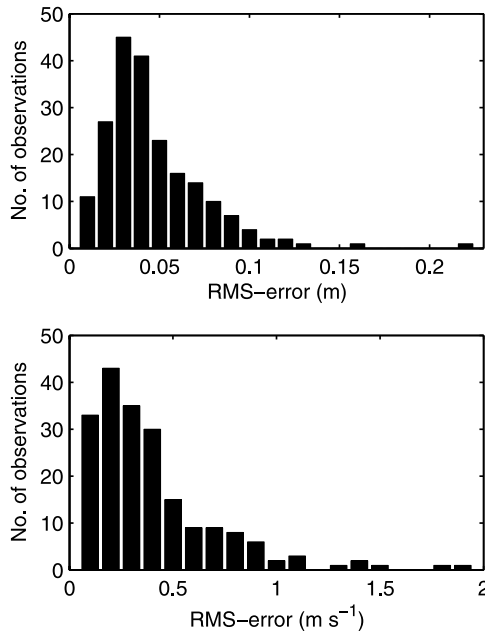


Figure 7. Frequency distributions of the RMS error between measurements and model predictions for each of the 214 swash events in the data set. Errors for (top) swash depth and (bottom) velocity.

1998; Raubenheimer, 2002]. The swash kinematics model predicts this general behavior (Figure 1) in agreement with the data obtained here (Figure 8). The correlation between the uprush and backwash data is positive but weak ($r = 0.39$), since T_u and T_b differ most at positions on the lower beach near the bore collapse point (i.e., where T_u is largest) and converge on the upper beach near the limit of shoreline excursion (i.e., where T_u is smallest). The low correlation is therefore also an indicator of the asymmetry in the swash kinematics. Model predictions for T_u versus T_b vary with

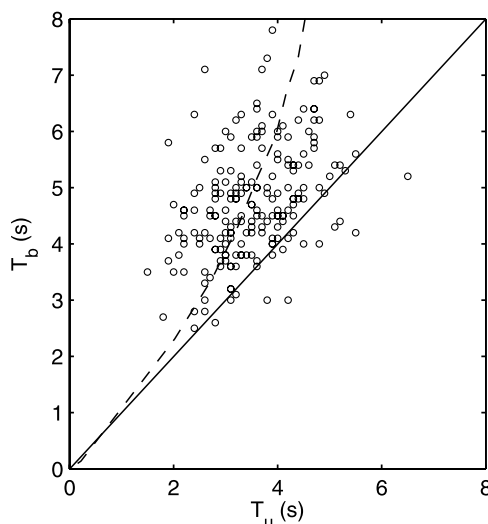


Figure 8. Durations of local uprush T_u plotted against backwash T_b . The solid line shows the 1:1 relationship, and the dashed line shows the model predictions for T_u versus T_b for a swash cycle typical of the data set ($T_s = 14$ s).

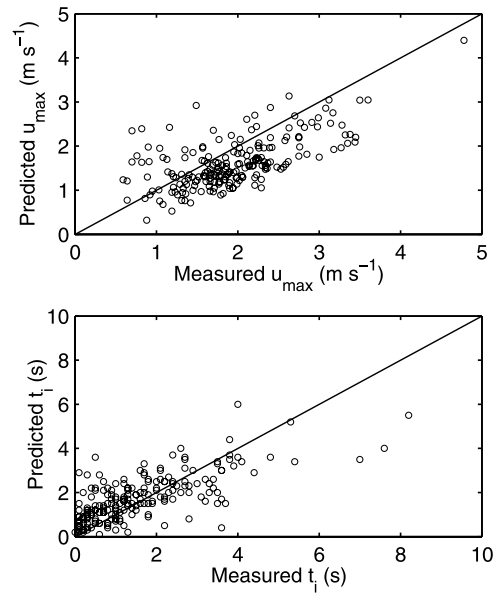


Figure 9. A comparison of measured and model predictions for the (top) magnitude and (bottom) timing of the maximum flow velocity in each swash event. The solid lines indicate the 1:1 relationship.

cross-shore location and are plotted on Figure 8 for a typical swash cycle (period 14s), showing good agreement with the data set.

[24] The peak or maximum flow velocity is an important parameter in some formulations for sediment transport rate [e.g., Masselink and Hughes, 1998]. For the swash events described here, this is equivalent to the shoreline velocity when it arrives at the ADV (i.e., the start of the swash event). Data and model predictions of the magnitude, u_{\max} , and timing, t_i , of the maximum flow velocity are compared in Figure 9. Again, model-data comparisons are relative to the time of bore collapse when the shoreline starts moving shoreward; that is, they include phase errors. There is a tendency for the model to underpredict the magnitude of the maximum velocity, but this is in part due to errors in estimating the exact distance from the point of bore collapse to the measurement location. The accuracy of the model is indicated by the RMS error between model predictions and data, which, in this case, is 0.62 m s^{-1} and 1.14 s for the maximum velocity and timing, respectively. Finally, the overall good agreement between the model and data suggests that the presence of infragravity energy in the swash (Figure 4) does not significantly degrade the model's predictive capabilities for individual swash events.

6. Discussion

[25] The swash model presented in section 3 has, in various stages of refinement, already been compared to field measurements of shoreline motion and water depth in previous studies [e.g., Waddell, 1976; Hughes, 1992; Holland and Puleo, 2001]. This is the first study, however, to compare the model to field measurements of Eulerian flow velocity. The model-data comparisons are encouraging, but the free parameters in the model warrant further discussion. First are the values of C and D in equation (11),

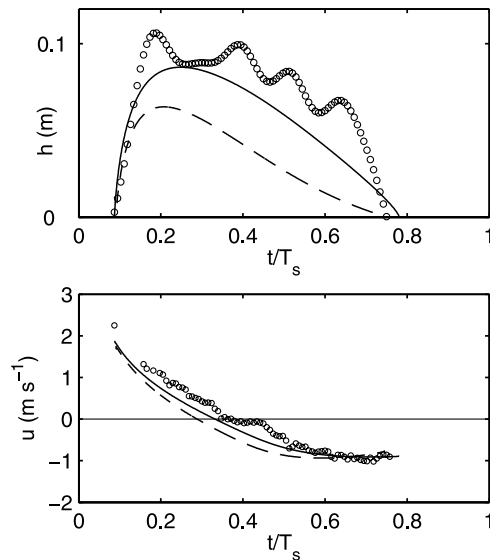


Figure 10. (top) Measured water depth h (open circles) and model predictions for the swash event shown in the top left corner of Figure 6. The model predictions are based on $D = 1$ (solid line) and $D = 2$ (dashed line). (bottom) Measured depth-averaged velocity u (open circles) for the same swash event replotted with the model predictions using $D = 1$ (solid line) and $D = 2$ (dashed line).

which is a semi-empirical function used to describe the time-varying water surface profile and water depth throughout the swash zone, beginning at the time of bore collapse. For a steep laboratory beach face, gradient 1:10, *Baldock and Holmes* [1997] found that $C = 0.75$ and $D = 2$ resulted in a good approximation to the shape of the swash lens. In this study, beach face gradient 1:23, a value of $D = 1$ produced the best results. As a result, a sensitivity analysis was performed to determine the influence of the choice of C and D on the predicted kinematics and swash depths.

[26] The parameter C controls the overall shape of the swash lens, with smaller values of C giving a more convex shape. The parameter D controls the rate of thinning of the swash lens, smaller values giving a slower decrease in water depth at a fixed point. The sensitivity analysis showed that the choice of C has relatively little effect on the velocity predictions, resulting in virtually no change in the time of flow reversal, and changes in the uprush and backwash velocities of order 10%. The model is more sensitive to the choice of D , with values closer to 1 giving greater flow depths and more uniform flow acceleration in the backwash and making the ratio T_u/T_b closer to 1. This is consistent with a more uniform water depth across the swash zone, typical of the swash on milder slopes. Figure 10 compares model predictions for $D = 1$ and $D = 2$ with data from the swash event shown in the top left-hand panel of Figure 6. For $D = 1$, the predicted maximum depth increases and occurs slightly later and the swash thins more slowly, giving greater water depths at the measurement location. Similarly, the depth-averaged velocity in the backwash is reduced and flow reversal is predicted to occur later in the swash cycle. While a number of parameters might affect the shape of the swash lens, beach slope is likely to be the most important

factor, since the flow is primarily controlled by the down-slope component of gravity. The results from the sensitivity analysis are consistent with this assumption.

[27] *Hughes* [1995] and *Puleo and Holland* [2001] found that a choice of δ_u in the model equal to the maximum swash depth occurring at the mid-swash position provided good estimates of the shoreline position, X . The same approach here is found to produce good estimates of the kinematics and flow depths. Nevertheless, it is appropriate to consider the sensitivity of the model results to δ_u . Using the same initial conditions used to generate Figure 1, Figure 11 shows the model predictions for Eulerian flow velocity at the mid-swash position for three different values of δ_u . The solid line shows the result based on setting δ_u equal to the maximum depth at the mid-swash position, i.e., by solving equations (4) and (11) iteratively. Increasing or decreasing δ_u from this value by 50% does not strongly impact on the results.

[28] The final free parameter, usually determined by calibration, is the friction factor, f . The grain size at the study site was 0.28 mm, which compares closely to the grain sizes at Duck, North Carolina, in a study of swash zone friction factors by *Puleo and Holland* [2001]. Using the same ballistic model for the shoreline motion as that presented here, but with fixed values of $\delta_u = 0.05$ m and $\delta_b = 0.03$ m, they obtained the following inferred values for the friction factor: $f_u = 0.0049$ – 0.0065 and $f_b = 0.027$ – 0.039 . In comparison, values of $f_u = 0.01$ and $f_b = 0.05$ gave the best fit to the data obtained in this study, approximately 1.5–1.75 times larger. The difference in f_u between the two studies is probably partly explained by the different values of δ_u . Here, equations (4) and (11) are solved iteratively to obtain a consistent value for δ_u , which for many of the swash events is greater than the constant 0.05 m used by

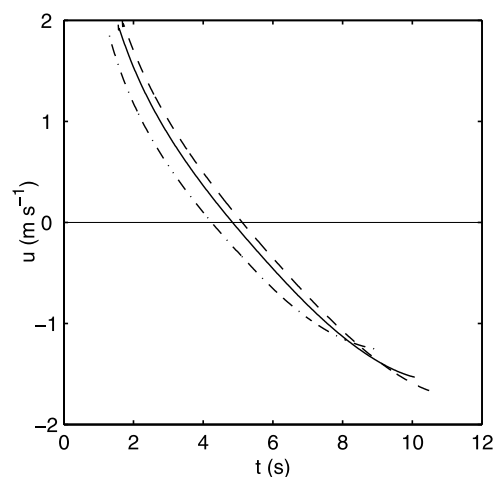


Figure 11. Model predictions of the Eulerian flow velocity for a swash event, located at the mid-swash position on the beach face. Initial conditions for the model are the same as those used to generate Figure 1, but comparing the effect of using different values for δ_u . The solid line shows the result recommended in this study (i.e., solving equations (4) and (11) iteratively to match δ_u to the maximum water depth at the mid-swash position). The dashed and dash-dotted lines show the effect of choosing a value that is 50% larger and 50% smaller, respectively.

Puleo and Holland [2001]. It is important to recognize from equation (3) that it is the ratio f/δ that determines the friction effects in the model; therefore the friction factors given by Puleo and Holland [2001] are only appropriate for their fixed choice of $\delta_u = 0.05$ m and $\delta_b = 0.03$ m. In addition, there are a number of other physical processes not explicitly accounted for in the ballistic swash model, which influence the swash dynamics, and thus model calibration, and which may also explain the disparity between the two studies. The effects of infiltration and pressure gradients, which are ignored in the model, are cases in point [Turner and Masselink, 1998; Puleo and Holland, 2001].

[29] In the model-data comparisons presented above, the velocity is undefined between individual swash events. This raises an interesting question regarding the interpretation of flow velocity data from the swash zone and any apparent local temporal acceleration observed at a fixed point on the beach, $a = \partial u / \partial t$. The ballistic swash model predicts that such accelerations are negative (seaward) throughout the swash event. This is consistent with the present data, where the largest flow velocities are the shoreline velocity as it passes the ADV location in both directions. It is fair to say that in those cases where the ADV was located close to the point of bore collapse (top panel in Figure 5 and several examples in Figure 6), we have no reliable information on the flow velocities immediately after the start of local uprush, due to the presence of excessive acoustic scatterers from the bore collapse process. In other cases, however, where the ADV was located farther away from the point of bore collapse (bottom panel in Figure 5 and several examples in Figure 6), there are sufficient data available to suggest that the Eulerian flow velocity decreases throughout the local uprush, and as the ballistic swash model suggests, there is no positive local acceleration. Petti and Longo [2001] present similar velocity data obtained using a laser Doppler velocimeter close to the start of local uprush, and there is also no evidence of strong, positive local accelerations in their published kinematic data.

[30] Although the data presented here show no evidence of positive (landward) local temporal accelerations in the swash zone, positive accelerations may occur during and close to the point of bore collapse, where strong pressure gradients potentially exist due to a landward sloping water surface. At this time the shoreline also experiences a strong positive convective acceleration ($U\partial U/\partial X$). Yeh and Ghazali [1988] show that this initial acceleration of the shoreline is extremely rapid, occurring over a very narrow distance and in a very short period of time. Data presented by Baldock and Holmes [1999] and Petti and Longo [2001] show that the time interval over which bore collapse and positive shoreline acceleration occurs is only about 5–10% of the total swash period, or 10–20% of T_u (see their Figures 3 and 7–9, respectively). The data and model predictions presented above are consistent with this, in that once the bore has fully collapsed, only negative (seaward) local acceleration occurs. The absence or presence of shoreward directed local accelerations in the swash zone has implications for sediment transport modeling, where recent work has focused on local flow acceleration as a potentially important factor [Nielsen, 2002; Puleo et al., 2003]. For swash forced by fully developed bores on intermediate-reflective beaches, such local accelerations

appear restricted to the seaward part of the swash zone, and therefore probably are not relevant to sediment transport modeling over the remainder of the beach face.

7. Conclusions

[31] The ballistic swash model originally proposed by Shen and Meyer [1963] to describe the shoreline motion, and subsequently refined to include friction [Kirkgöz, 1981; Hughes, 1995; Puleo and Holland, 2001], has been further developed to calculate the internal swash kinematics. The model predictions are compared to over 200 field observations of individual, non-interacting swash events on an intermediate-reflective beach. Model predictions for Eulerian flow velocities, flow depths, and flow durations compare well with the field measurements, which cover different relative positions within the swash zone. In particular, the timing and magnitude of the maximum predicted flow velocity at a fixed location on the beach face matches well with the measured shoreline velocity upon its arrival at that location. Flow depths are well predicted, together with the cross-shore variation in uprush and backwash durations. Detailed comparisons of Eulerian velocity time series from individual swash events compare very well with the data, both in terms of velocity magnitude and the time of flow reversal. The timing of the zero velocity crossing in a local swash event is correctly predicted to occur prior to the time the shoreline reaches its maximum landward displacement; thus the flow duration of the local uprush is noticeably less than the flow duration of the local backwash in both model predictions and observations. Finally, the data show no positive (shoreward directed) local accelerations, $\partial u / \partial t$, in the flow velocity at a fixed point during either uprush or backwash. This is consistent with the ballistic swash model and relevant to sediment transport modeling in the swash zone.

[32] **Acknowledgments.** This research was funded by the Australian Research Council (grants A10009206 and LX0454743) and UQ grants 2002001540 and 20033000318. Field assistance from David Mitchell, Aaron Coutts-Smith, Peter Nielsen, Matt Tomkins, and Nick Cartwright is greatly appreciated. Helpful comments and suggestions by two anonymous reviewers helped to improve the paper.

References

- Baldock, T., and P. Holmes (1997), Swash hydrodynamics on a steep beach, in *Coastal Dynamics '97*, edited by E. B. Thornton, pp. 784–793, Am. Soc. of Civ. Eng., Reston, Va.
- Baldock, T. E., and P. Holmes (1999), Simulation and prediction of swash oscillations on a steep beach, *Coastal Eng.*, **36**, 219–242.
- Butt, T., and P. Russell (1999), Suspended sediment transport mechanisms in high-energy swash, *Mar. Geol.*, **161**, 361–375.
- Butt, T., and P. Russell (2000), Hydrodynamics and cross-shore sediment transport in the swash-zone of natural beaches: A review, *J. Coastal Res.*, **16**, 255–268.
- Elfrink, B., and T. E. Baldock (2002), Hydrodynamics and sediment transport in the swash zone: A review and future perspectives, *Coastal Eng.*, **45**, 149–167.
- Elgar, S., B. Raubenheimer, and R. T. Guza (2001), Current meter performance in the surf zone, *J. Atmos. Oceanic Technol.*, **18**, 1735–1746.
- Freeman, J. C., and B. LeMehaute (1964), Wave breakers on a beach and surges on a dry bed, *Proc. Am. Soc. Civ. Eng.*, **90**, 187–216.
- Hibberd, S., and D. H. Peregrine (1979), Surf and run-up on a beach: A uniform bore, *J. Fluid Mech.*, **95**, 245–323.
- Ho, D. V., R. E. Meyer, and M. C. Shen (1963), Long surf, *J. Mar. Res.*, **21**, 219–230.
- Holland, K. T., and J. A. Puleo (2001), Variable swash motions associated with foreshore profile change, *J. Geophys. Res.*, **106**, 4613–4623.

- Holland, K. T., B. Raubenheimer, R. T. Guza, and R. A. Holman (1995), Run-up kinematics on a natural beach, *J. Geophys. Res.*, **100**, 4985–4993.
- Holman, R. A., and R. T. Guza (1984), Measuring run-up on a natural beach, *Coastal Eng.*, **8**, 129–140.
- Hughes, M. G. (1989), A field study of wave-sediment interaction in the swash zone, Ph.D. thesis, 249 pp., Univ. of Sydney, Sydney.
- Hughes, M. G. (1992), Application of a non-linear shallow water theory to swash following bore collapse on a sandy beach, *J. Coastal Res.*, **8**, 562–578.
- Hughes, M. G. (1995), Friction factors for wave uprush, *J. Coastal Res.*, **11**, 1089–1098.
- Hughes, M. G., G. Masselink, D. Hanslow, and D. Mitchell (1997), Toward a better understanding of swash zone sediment transport, in *Coastal Dynamics '97*, edited by E. B. Thornton, pp. 804–813, Am. Soc. of Civ. Eng., Reston, Va.
- Kemp, P. H. (1975), Wave asymmetry in the nearshore zone and breaker area, in *Nearshore Sediment Dynamics and Sedimentation*, edited by J. Hail and A. Carr, pp. 47–67, John Wiley, Hoboken, N. J.
- Kirkgöz, M. S. (1981), A theoretical study of plunging breakers and their run-up, *Coastal Eng.*, **5**, 353–370.
- Kobayashi, N., and A. Wurjanto (1992), Irregular wave setup and run-up on beaches, *J. Water Port Coastal Ocean Eng.*, **118**, 368–386.
- Larson, M., and T. Sunamura (1993), Laboratory experiment on flow characteristics at a beach step, *J. Sed. Petrol.*, **63**, 495–500.
- Masselink, G., and M. G. Hughes (1998), Field investigation of sediment transport in the swash zone, *Cont. Shelf Res.*, **18**, 1179–1199.
- Nielsen, P. (2002), Shear stress and sediment transport calculations for swash zone modeling, *Coastal Eng.*, **45**, 53–60.
- Osborne, P. D., and G. A. Rooker (1999), Sand re-suspension events in a high energy infragravity swash zone, *J. Coastal Res.*, **15**, 74–86.
- Peregrine, D. H., and S. M. Williams (2001), Swash overtopping a truncated plane beach, *J. Fluid Mech.*, **440**, 391–399.
- Petti, M., and S. Longo (2001), Turbulence experiments in the swash zone, *Coastal Eng.*, **43**, 1–24.
- Puleo, J. A., and K. T. Holland (2001), Estimating swash zone friction coefficients on a sandy beach, *Coastal Eng.*, **43**, 25–40.
- Puleo, J. A., K. T. Holland, N. G. Plant, D. N. Slinn, and D. M. Hanes (2003), Fluid acceleration effects on suspended sediment transport in the swash zone, *J. Geophys. Res.*, **108**(C11), 3350, doi:10.1029/2003JC001943.
- Raubenheimer, B. (2002), Observations and predictions of fluid velocities in the surf and swash zones, *J. Geophys. Res.*, **107**(C11), 3190, doi:10.1029/2001JC001264.
- Raubenheimer, B., and R. T. Guza (1996), Observations and predictions of runup, *J. Geophys. Res.*, **101**, 25,575–25,588.
- Raubenheimer, B., R. T. Guza, S. Elgar, and N. Kobayashi (1995), Swash on a gently sloping beach, *J. Geophys. Res.*, **100**, 8751–8760.
- Raubenheimer, B., S. Elgar, and R. T. Guza (2004), Observations of swash zone velocities: A note on friction coefficients, *J. Geophys. Res.*, **109**, C01027, doi:10.1029/2003JC001877.
- Shen, M. C., and R. E. Meyer (1963), Climb of a bore on a beach: 3. Run-up, *J. Fluid Mech.*, **16**, 113–125.
- Turner, I. L., and G. Masselink (1998), Swash infiltration-exfiltration and sediment transport, *J. Geophys. Res.*, **103**, 30,813–30,824.
- Waddell, E. (1976), Swash-groundwater-beach profile interactions, in *Beach and Nearshore Sedimentation*, edited by R. A. Davis Jr. and R. L. Ethington, pp. 115–125, Soc. of Econ. Paleontol. and Mineral., Tulsa, Okla.
- Wright, L. D., and A. D. Short (1984), Morphodynamic variability of surf zones and beaches: A synthesis, *Mar. Geol.*, **56**, 93–118.
- Yeh, H. H., and A. Ghazali (1988), On bore collapse, *J. Geophys. Res.*, **93**, 6930–6936.
- Yeh, H. H., A. Ghazali, and I. Marton (1989), Experimental study of bore run-up, *J. Fluid Mech.*, **206**, 563–578.

T. E. Baldock, Department of Civil Engineering, University of Queensland, Brisbane, QLD 4072, Australia.

M. G. Hughes, School of Geosciences, University of Sydney Institute of Marine Science, Edgeworth David Building (FO5), University of Sydney, NSW 2006, Australia. (michaelh@mail.usyd.edu.au)